

Extrapolated Boundary Element Method for Three-Dimensional Inductance Calculation

M. HOSOYA

*Department of Information Science, Faculty of Science,
University of Tokyo, Tokyo, Japan*

E. GOTO

*Department of Information Science, Faculty of Science,
University of Tokyo, Tokyo, Japan and
Information Science Laboratory, The Institute of
Physical and Chemical Research, Saitama, Japan*

AND

T. SOMA

*Information Science Laboratory, The Institute of
Physical and Chemical Research, Saitama, Japan*

Received July 29, 1986; revised January 30, 1987

In the case of a nearly perfect conductor, i.e., when the skin depth δ (in ordinary conductors) or the London penetration depth δ_L (in superconductors) is much smaller than the other physical scales, the current flows only on the surface. Hence, the three-dimensional distribution of the magnetic field is fully specified by the two-dimensional current distribution (boundary elements) on the surface. The specific BEM (boundary element method) is called SCM (surface current method). In SCM, the surface is partitioned into N small areas, each with a looping current I_i ($1 \leq i \leq N$). I_i 's are determined by solving N simultaneous linear equations so as to eliminate the normal component of the magnetic field at the center of each area. The inductance is given in terms of the magnetic energy among N current loops. Thus, the problem is reduced to a two-dimensional one in SCM. To obtain the final results, the error estimate as a function of N is made and they are obtained as the extrapolation for N tending to infinity. Calculations for some examples including a fully three-dimensional object are presented. The effect of non-zero δ and δ_L can be, in the present SCM, made by thinning the object by the amount δ (if the width of the conductor is larger than δ) but the more rigorous treatment is left for future study. © 1988 Academic Press, Inc.

1. INTRODUCTION

The computation of inductance is very important for the design of circuitry and devices in Josephson junction technology, and various methods for inductance calculation are derived [1-3]. However, by these methods, when the current

distribution is three-dimensional, the calculation becomes impossible because the requirements for the computation time or memory is too severe in the current state.

In the case of a nearly perfect conductor, i.e., when the skin depth δ or the London penetration depth δ_L is much smaller than the other physical scales, the conductor is assumed to be perfect, and the current is assumed to flow only on the surface. Hence, the magnetic field of the system is fully specified by the two-dimensional current distribution on the surface.

If three-dimensional field problem is solved by computing the two-dimensional current distribution (boundary elements) on the surface, the requirements for computational resources are much reduced, which enables the calculation of an object with more complex shape. In this paper, a new variant of BEM, called the *surface current method* (SCM) which follows the above scheme, is introduced. Calculations for some examples including a fully three-dimensional object are presented. The error of SCM is discussed in relation to the influence of the extrapolation, which is used in order to obtain the final result effectively.

2. PRINCIPLES OF SCM

In SCM, the surface is partitioned into N small areas, each with a looping current I_i ($1 \leq i \leq N$). Let the normal component of the magnetic field at the center of looping current I_i be H_i . Then, H_i can be written as the linear combination of I_i as shown in (1).

$$H_i = \sum_{j=0}^N a_{ij} I_j, \tag{1}$$

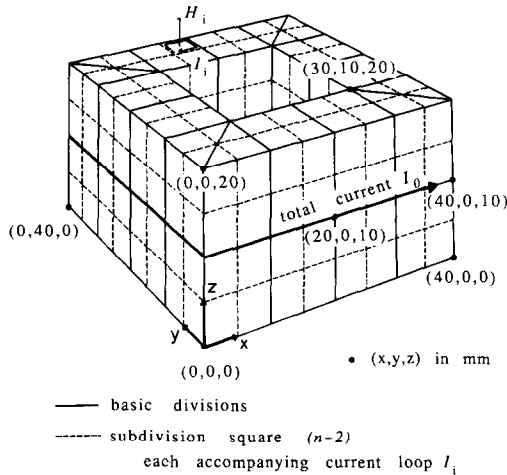


FIG. 1. Divisions of the surface of a square block. Divisions of the surface of a square block are illustrated. I_0 flows on the outer surface in this figure. Coordinates of Fig. 1 correspond to those of Fig. 2.

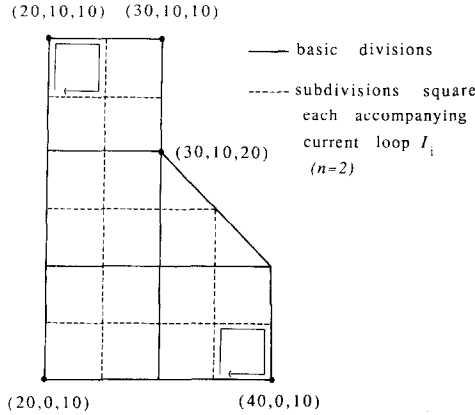


FIG. 2. Subdivisions of the surface of the square block. Each subdivision has a current loop.

where a_{ij} is a constant determined by the shape of the conductor and can be calculated directly from the positions of I_i and I_j . I_0 is any current path flowing the whole conductor (see Figs. 1, 2). Because the current is redistributed by the condition described below, there is no restriction on the path where I_0 flows even if it is chosen to flow the whole conductor. H_i must be 0 because the conductor is perfect. Hence, I_i can be obtained by solving the simultaneous linear equations (2).

$$\begin{bmatrix} 1 & 0 & \cdot & 0 \\ a_{10} & \vdots & \cdot & \vdots \\ \vdots & a_{ij} & \cdot & \vdots \\ \vdots & \vdots & \cdot & a_{NN} \end{bmatrix} \cdot \begin{bmatrix} I_0 \\ I_1 \\ \vdots \\ I_N \end{bmatrix} = \begin{bmatrix} I \\ 0 \\ \vdots \\ 0 \end{bmatrix} \tag{2}$$

where I is the current of the source.

The inductance L is given in terms of the magnetic field energy among current loops as shown in (3).

$$L = \frac{1}{I^2} \sum_{i,j} M_{ij} I_i I_j, \tag{3}$$

where M_{ij} is the mutual inductance between current loops i and j , and can be calculated directly from the positions of the current loops.

Therefore, the inductance of a three-dimensional object is reduced to a two-dimensional one in SCM, which may be regarded as a special case of BEM.

3. EXTRAPOLATION ERROR OF SCM

In SCM, the surface is divided into N_0 basic divisions at first. Then, each basic division is subdivided into n subdivisions for each dimension. That is, total number

of subdivisions, N , is $N_0 n^2$ for a three-dimensional object. The calculation is performed for various n 's and the results are extrapolated to obtain the final inductance. The reason why the surface is divided in two steps (basic and sub) is for increasing the effectiveness of the extrapolation. In FEM (finite element method), the element division is executed mainly by experience. By this method, the shape of elements has irregularity, which decreases the effectiveness of extrapolations. In SCM, because such irregularity is absorbed by the basic divisions and the extrapolation is performed on the regular subdivisions, it is expected to work more effectively.

The extrapolation enables the effective anticipation of the true inductance, i.e., the value at $n = \infty$. If the inductance can be computed from relatively small n 's, much time and memory for the calculation can be reduced.

In the following, the extrapolation and the error of extrapolation are considered.

3.1. Extrapolation and the Error Polynomial

If the number of subdivision n is an integer, we can only use the following n sampling points to obtain an unknown value,

$$f(n), f(n-1), f(n-2), \dots, f(1).$$

Let $x = 1/n$. We must anticipate the extrapolated value at $x = 0$ ($n = \infty$) effectively. If the original function is a polynomial of degree k in x , the exact value can be obtained from the following $k+1$ points,

$$f(n), f(n-1), f(n-2), \dots, f(n-k).$$

We use the polynomial defined from the above $k+1$ points as an extrapolation polynomial $P_{n,k}$. Hence,

$$P_{n,k}(\lambda_i f(n-i); x) = \frac{1}{k!} \sum_{i=0}^k (-1)^i \binom{k}{i} (n-i)^k f(n-i) \prod_{\substack{j=0 \\ j \neq i}}^k (1 - (n-j)x). \quad (4)$$

The error polynomial is defined as

$$Z_{n,k}(\lambda_i f(n-i)) \equiv P_{n,k}(\lambda_i f(n-i); 0) \quad (5.1)$$

$$= \frac{1}{k!} \sum_{i=0}^k (-1)^i \binom{k}{i} (n-i)^k f(n-i) \quad (5.2)$$

$$= \frac{1}{k!} \Delta_n^k (n^k f(n)), \quad (5.3)$$

where

$$\Delta_n f(n) = f(n) - f(n-1) \quad (6.1)$$

$$\Delta_n^{k+1} f(n) = \Delta_n^k \cdot \Delta_n f(n). \quad (6.2)$$

If f is decomposed into two parts as

$$f(n) = \sum_{i=0}^k a_i n^{-i} + g(n)$$

then

$$Z_{n,k}(\lambda_i f(n-i)) = \frac{1}{k!} \Delta_n^k(n^k f(n)) \tag{7.1}$$

$$= \frac{1}{k!} \sum_{i=0}^k a_i \Delta_n^k(n^{k-i}) + \frac{1}{k!} \Delta_n^k(n^k g(n)) \tag{7.2}$$

$$= a_0 + Z_{n,k}(\lambda_i g(n-i)) \tag{7.3}$$

because

$$\Delta_n^k(n^{k-m}) = 0 \quad (1 \leq m \leq k). \tag{8}$$

Hence, $Z_{n,k}(\lambda_i g(n-i))$ is the error from $a_0 = f(\infty)$. In Table I, the results of the calculation $Z_{n,k}(\lambda_i g(n-i))$ are summarized for the various forms of g . We can analyze the error by changing k, n and examining which type the original function may be.

3.2. Round-off Error

If each f_i contains an error by ε ,

$$|Z_{n,k}| \leq \frac{\varepsilon}{k!} \sum_{i=0}^k \binom{k}{i} (n-i)^k. \tag{9}$$

Therefore, maximum of k, k_{\max} is determined by (10):

$$\max |Z_{n,k}| < \delta; \tag{10}$$

TABLE I
 $Z_{n,k}$ for Various $g(n)$'s

$g(n)$	$Z_{n,k}(n \gg k)$
$\frac{1}{n^{k+j}}$	${}_{k+j-1}C_k \frac{(-1)^k}{n^{k+j}}$
$\frac{1}{n^j} \log n$	$\frac{(-1)^{j-1}}{{}_k C_j j n^j}$
$n^{1/j}$	$\left(\frac{e}{kn}\right)^{1/j} (k \gg 1)$

TABLE II
 k_{\max} Determined by the Round-off Error

n	$\varepsilon = 16^{-6}$			$\varepsilon = 16^{-14}$			
	$\delta = 10^{-2}$	$\delta = 10^{-3}$	$\delta = 10^{-4}$	$\delta = 10^{-2}$	$\delta = 10^{-4}$	$\delta = 10^{-6}$	$\delta = 10^{-8}$
	8	8	8	4	8	8	8
12	7	4	3	12	12	12	12
16	5	3	2	16	16	16	16
20	3	3	2	20	20	20	11
24	4	3	2	24	24	13	9
28	3	2	2	20	16	11	7
32	2	2	1	18	13	10	7

ε is caused by the round-off error and varies according to the precision of a number. δ is the maximum (absolute) error to be permitted. In Table II, k_{\max} is calculated for some cases. As shown in Table II, k must not be so large.

3.3. Singularity of $g(n)$

If $g(n)$ has a singular point at n_0 such as

$$g(n) = \frac{1}{n - n_0}, \tag{11}$$

then

$$|Z_{n,k}(\lambda_i g(n-i))| = \frac{1}{k!} \Delta_n^k \left(\frac{n^k}{n - n_0} \right). \tag{12}$$

If k becomes too close to n , the value of (12) increases. When $n_0 = 1$, k_{opt} which optimize (12) is shown in Table III. This is the second reason that k should not be so large.

TABLE III
 k_{opt} when $g(n)$ Has a Pole

n	k_{opt}
8	6
12	4
16	3
20	3
24	2
28	2
32	2

4. SOME EXAMPLES

Based on the analysis considered in the previous section, the error analyses are performed on some examples. The results are compared to the experimental data or a theoretical value. The results of these error analyses indicate the accuracy of the calculation by SCM.

4.1. Annulus

The first example is the inductance of the thin annulus shown in Fig. 3. If r_2 is infinite, the inductance is given by (13):

$$L = 2r_1 \mu, \tag{13}$$

where μ is the permeability of the conductor. The annulus is subdivided into n small areas in radial direction. Because of the rotational symmetry, the problem is reduced to a one-dimensional one. Mutual inductance between two current segment loops is given by (14) and (15).

$$M_{ij} = 2\mu \frac{(R_i R_j)^{1/2}}{k} \left\{ \left(1 - \frac{k^2}{2} \right) K(k) - E(k) \right\} \tag{14}$$

$$k^2 = \frac{4R_i R_j}{(R_i + R_j)^2}, \tag{15}$$

where R_i, R_j is the radius of each loop and $K(k), E(k)$ are complete elliptic integrals of the first and second kind. The inductance calculation is done for various r_2 's and n 's. The results are extrapolated in both directions and compared to (13). They are

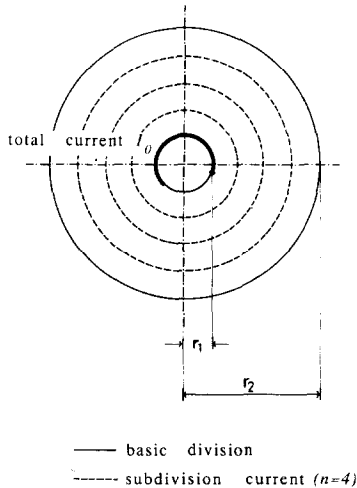


FIG. 3. Thin annulus. If r_2 is infinite, the inductance can be calculated analytically.

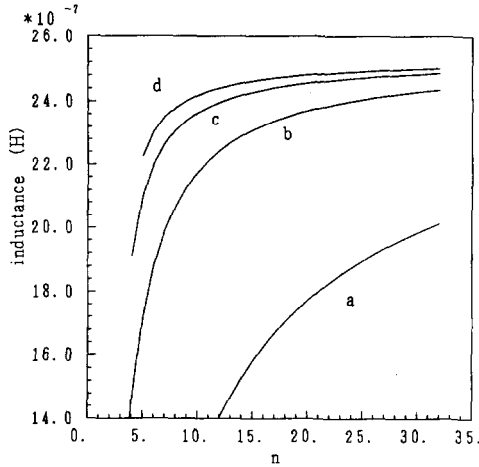


FIG. 4. Inductance of the thin annulus is calculated and extrapolated for r_2 and n . As for r_2 direction, the values are extrapolated by the quadratic polynomial. As for n direction, the results are extrapolated by the polynomials of $1/n$. a is the values without extrapolation; b, c, and d are the values extrapolated by the polynomials of -1 , -2 , and -3 degree in n , respectively.

summarized in Figs. 4 and 5, where $r_1 = 1$ and the extrapolation for r_2 is performed by the quadratic polynomial determined by 3 points at $r_2 = 1, 2, 4$. As shown in Fig. 5, the inductance is obtained with 1% relative error at $n \geq 19$ by the extrapolation polynomial of degree -3 in n . The slope of a line in Fig. 5 indicates the exponent of the primarily contributing term in $Z_{n,k}$. The slope is smaller than $-(i+1)$ when the highest exponent of the extrapolating function is $-i$. This fact indicates the existence of the term with the smaller exponent in the extrapolating function.

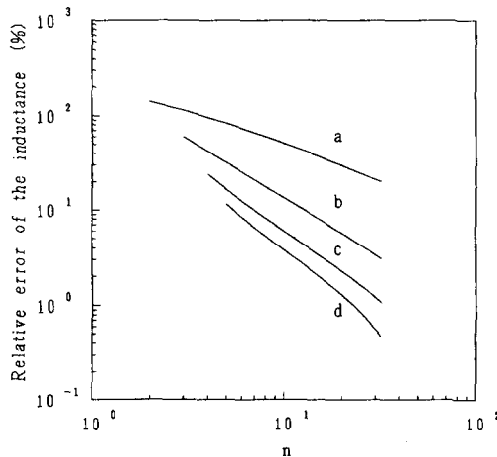


FIG. 5. Relative error of the inductance of the thin annulus. Results of Fig. 4 are compared to the analytical value, and the errors are plotted. Curve numbers correspond to those of Fig. 4.

4.2. Parallel Thin Plates

A second example is the inductance of infinitely long, parallel thin plates shown in Fig. 6. Current of two plates are the same and the direction is reversed. The inductance is given by (16).

$$L = \mu \frac{K(k)}{K'(k)}, \tag{16}$$

where $K'(k)$ is the complementary function of $K(k)$. In order to avoid the divergence of the inductance, calculations are performed for the current segments with finite spacing. The influence of this finite spacing is $O((1/n) \log n)$ and can be eliminated by the extrapolation. In Fig. 7, convergence for various extrapolating functions are plotted.

4.3. Square Block with a Square Hole

The last example is the inductance of a square block with a square hole shown in Fig. 1. (Sub)divisions of the object are also shown in Figs. 1 and 2. Mutual inductance between two current segments is calculated by the equations described in the Appendix. Current distribution on the surface is plotted in Fig. 8. At line α_1 , 66% of the whole current flows on the inner surface, 28% on the upper (lower) surface, and the rest on the outer surface. At line α_2 , 76% of the whole current flows on the inner surface, 21% on the upper (lower) surface, and the rest on the outer surface. Therefore, 10% flows into the inner surface from the upper (lower) surface between line α_1 and α_2 . The current density increases near the corner. The inductance $L(n)$ is plotted in Fig. 9. $\Delta_n(L(n))$ is shown in Fig. 10, which is almost equal to $dL(n)/dn$. Figure 10 indicates that the primary contributing term of $L(n)$ is n^{-1} . Therefore, $L(n)$ is extrapolated by the polynomial of degree -1 in n . The extrapolated value $a_0 + \Delta_n(nL(n))$ and its differential value $\Delta_n^2(nL(n))$ are plotted also in Figs. 9 and 10.

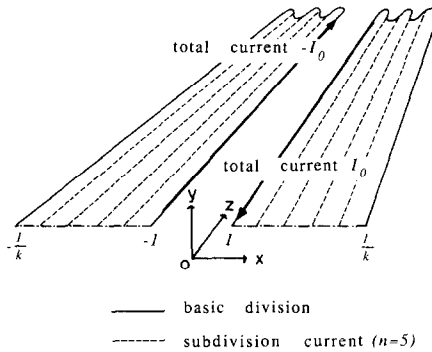


FIG. 6. Parallel thin plates. Inductance of this system can be obtained analytically. In SCM, the calculations are performed for current segments with finite spacing to avoid the divergence of the mutual inductance between the segments.

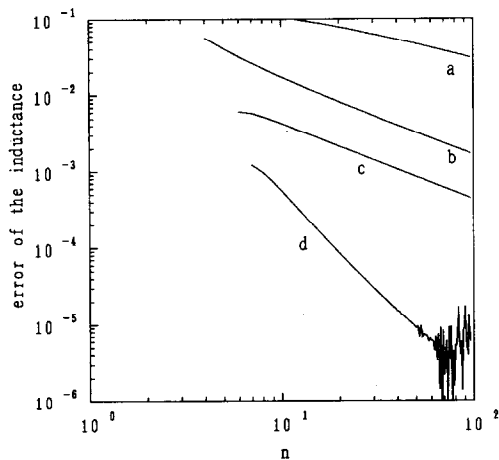


FIG. 7. Inductance of the parallel thin plates. The results of the calculation are extrapolated by various functions. a is the value without extrapolation (L). b is $\Delta_n(n \Delta_n(nL))$ by which $1/n$, $(1/n) \log n$ terms are eliminated. c is $\frac{1}{4} \Delta_n^2(n^2 \Delta_n^2(n^2L))$ by which $1/n^2$, $1/n$, $(1/n^2) \log n$, $(1/n) \log n$ terms are eliminated. In d $1/n^2$, $1/n$, $(1/n^2) \log n$, $(1/n) \log n$, $(1/n)(\log n)^2$ terms are eliminated.

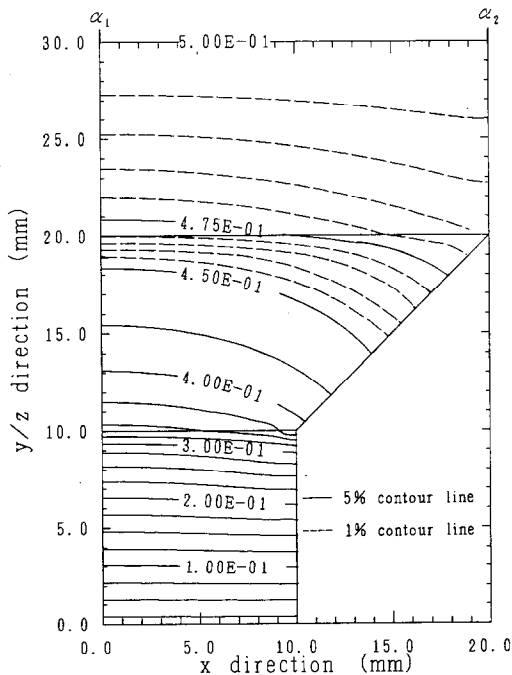


FIG. 8. Current distribution of the square block of Fig. 1 is shown. Almost all current flows on the inner surface.

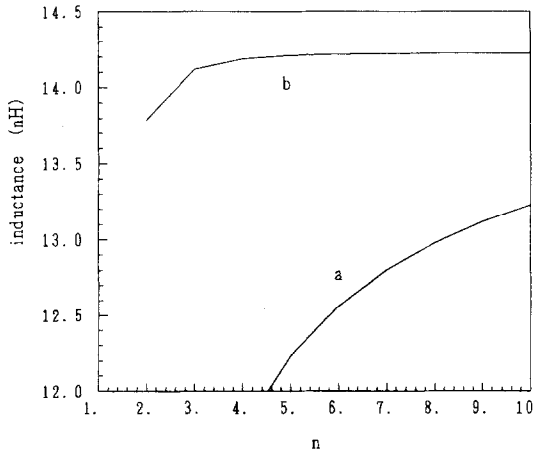


FIG. 9. Inductance of the square block is calculated (a) and extrapolated by the polynomial of -1 degree in n (b).

As shown in Fig. 10, $A_n^2(nL(n)) \approx 50n^{-5}$. Therefore, $A_n(nL(n)) \approx 10n^{-4}$ and the extrapolation error is about 10^{-3} at $n = 10$ which corresponds to less than 0.01% relative error.

The inductance measurement is actually performed on the model in the condition that the current frequency is 32 MHz [4]. In the case, δ is 11.6 μm and the conductor is assumed to be perfect. The measured inductance is 14.2 nH which agrees with the calculation completely.

The computational complexity of the computation is $O(n^4)$ to calculate H_i , $O(n^4)$ to calculate M_{ij} , and $O(n^6)$ to solve the simultaneous linear equation. However,

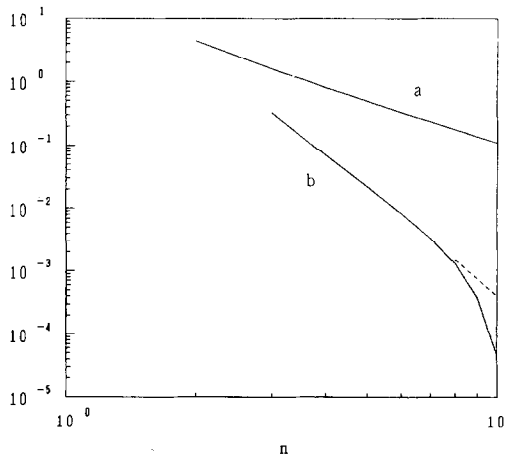


FIG. 10. Error of the inductance of the square block. Because $A_n(L) \approx O(n^{-2})$, L is extrapolated by the polynomial of -1 degree in n . Differential of the error polynomial, $A_n^2(nL) \approx O(n^{-5})$.

TABLE IV

Effect of δ_L

Penetration (%)	Rigorous treatment (pH/ μ m)	Thinning Approximation (pH/ μ m)	Relative error (%)
0	0.31740	0.31740	0
10	0.33917	0.34001	0.25
20	0.36203	0.36493	0.80
30	0.38718	0.39283	1.46
40	0.41542	0.42468	2.23
50	0.44782	0.46201	3.17
60	0.48516	0.50735	4.57
70	0.52790	0.56540	7.10
80	0.57640	0.64725	12.29
90	0.63085	0.78610	24.61

because actual n 's are small and because it is unnecessary to calculate M_{ij} when two current segments are vertical, the most costly calculation is H_i . When $n = 10$ and $N = 455$, CPU time to obtain the current distribution (set the matrix elements and solve it) is about 15 min, and to compute the inductance is about 10 min by Fujitsu M380.

5. THE EFFECT OF δ_L

In the case of an actual conductor, the inductance increases in comparison to the case where the conductor is assumed to be perfect, because the London penetration depth δ_L is not 0. For the system consisting of two parallel planes of infinite extent or of two coaxial conductors, the effect of δ_L is the same as considering the system having larger gaps obtained by thinning both conductors by the amount δ_L , because by definition the effect of δ_L is the same as though the current is concentrated at the plane δ_L from the surface. As one of the rough estimates let us consider the thinning effect for the two-dimensional transmission line system shown in Fig. 10 which may be one of the worst cases. Table IV shows the results of calculation, one for the proper treatment of δ_L and the other for a thinned system with $\delta_L = 0$ (the program used is described in [2]). In this case, agreement is acceptable for a small penetration. The error evaluation of the approximation for other configurations and more rigorous treatment for large penetration are left for future study.

6. CONCLUDING REMARKS

In the case of a nearly perfect conductor, the current flows only on the surface. Hence, the magnetic field of the system is fully specified by the two-dimensional

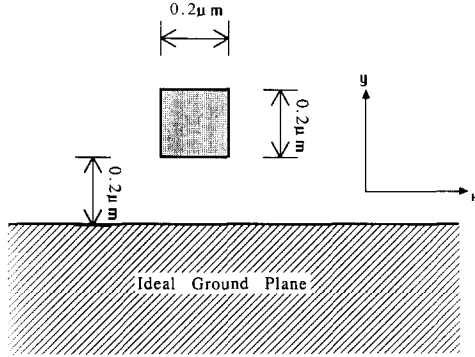


FIG. 11. Superconducting stripline. Effect of δ_L is estimated for the special case of superconducting stripline system. This system may be one of the worst case because if penetration is 100%, the thinning approximation diverges.

current distribution on the surface. In SCM, the surface is partitioned into N small areas, each with a looping current I_i ($1 \leq i \leq N$). I_i 's are determined by solving N simultaneous linear equations so as to eliminate the normal component of the magnetic field at the center of each area. The inductance is given in terms of the magnetic energy among N current loops. Therefore, the inductance of a three-dimensional object is reduced to a two-dimensional one in SCM, which enables the inductance calculation of an object with more complex shape.

In SCM, extrapolations are used to obtain the final result from small N 's. By the extrapolation, the precision of the computation increases drastically. Moreover, the error estimate becomes possible by examining the extrapolation polynomial.

Reduction to a two-dimensional problem and the use of extrapolations save much computational resources. When calculating the model shown in Fig. 11 with the accuracy of 0.66% error, SCM only needs 0.3% CPU time and 1.6% memory space by the method described in [2] (most of the saving seems to come from extrapolations).

Calculation for a fully three-dimensional object agrees well with experimental datum. More rigorous treatment of the δ_L effect is left for future study. Calculation of the δ_L effect within the scheme of present SCM is in progress.

APPENDIX I: EVALUATION OF MUTUAL INDUCTANCE INTEGRAL

Mutual inductance integral between two lines:

$$P_1(x_1, y_1, z_1) \rightarrow P_2(x_2, y_2, z_3) \quad \text{and} \quad P_3(x_3, y_3, z_3) \rightarrow P_4(x_4, y_4, z_4)$$

is given by

$$M = \int_0^{r_{12}} du \int_0^{r_{34}} dv \frac{c}{r(u, v)},$$

where c is the cosine of the angle between $\mathbf{P}_1\mathbf{P}_2$ and $\mathbf{P}_3\mathbf{P}_4$, $r(u, v)$ is the distance between $P_1 + \mathbf{P}_1\mathbf{P}_2(u/r_{12})$ and $P_3 + \mathbf{P}_3\mathbf{P}_4(v/r_{34})$, and r_{ij} is the distance between P_i and P_j . Hence,

$$c = \frac{(P_1 - P_2)(P_3 - P_4)}{r_{12}r_{34}}$$

$$r(u, v) = (u^2 + v^2 + r_{13}^2 - 2cuw - 2b_1u - 2b_2v)^{1/2},$$

where

$$b_1 = \frac{(P_2 - P_1)(P_3 - P_1)}{r_{12}}$$

$$b_2 = \frac{(P_4 - P_3)(P_1 - P_3)}{r_{34}}.$$

Let d be the minimum distance between the above two lines extended to infinity. In the following, the evaluation of M is classified according to the value of c and d .

AI.1. *In the nonparallel case, $|c| \neq 1$. In this case,*

$$d = r(u_0, v_0)$$

$$r(u, v) = r_0(u - u_0, v - v_0),$$

where

$$\begin{pmatrix} u_0 \\ v_0 \end{pmatrix} = \frac{1}{1 - c^2} \begin{pmatrix} 1 & c \\ c & 1 \end{pmatrix} \begin{pmatrix} b_1 \\ b_2 \end{pmatrix}$$

$$r_0(x, y) = (x^2 + y^2 - 2cxy + d^2)^{1/2}.$$

Therefore,

$$M = \int_{-u_0}^{r_{12}-u_0} dx \int_{-v_0}^{r_{34}-v_0} dy \frac{c}{r_0(x, y)}.$$

The above integral is given by the indefinite integral

$$\int dx \int dy \frac{c}{r_0(x, y)} = g(x, y) + h(x, y),$$

where

$$g(x, y) = \int dx \int dy \left(\frac{c}{r_0(x, y)} + \frac{cd^2}{r_0(x, y)^3} \right)$$

$$= y \log(x - cy + r_0(x, y)) + x \log(y - cx + r_0(x, y))$$

$$\begin{aligned}
 h(x, y) &= \int dx \int dy \frac{-cd^2}{r_0(x, y)^3} \\
 &= \frac{cd}{s} \arctan \frac{sr_0(x, y) d}{xys^2 + cd^2} \\
 &= \frac{cd}{s} \text{ATAN } 2(sr_0(x, y) d, xys^2 + cd^2) \\
 s &= (1 - c^2)^{1/2}.
 \end{aligned}$$

In numerical calculation, the FORTRAN function ATAN 2 should be used for proper branch selection of the arctan function. Hence,

$$\begin{aligned}
 M &= g(r_{12} - u_0, r_{34} - v_0) + g(-u_0, -v_0) - g(r_{12} - u_0, -v_0) - g(-u_0, r_{34} - v_0) \\
 &\quad + h(r_{12} - u_0, r_{34} - v_0) + h(-u_0, -v_0) - h(r_{12} - u_0, -v_0) - h(-u_0, r_{34} - v_0).
 \end{aligned}$$

AI.2. In the (anti)parallel case, $|c| = 1$.

From Fig. 12 and the definitions of b_1 and b_2 , we see the identity

$$\begin{aligned}
 b_2 &= -cb_1 \\
 r(u, v) &= ((u - c(v - b_2))^2 + d^2)^{1/2} \\
 d^2 &= r_{13}^2 - b_1^2.
 \end{aligned}$$

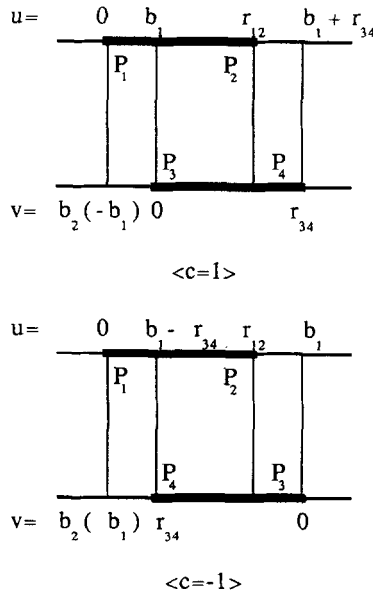


FIG. 12. Diagrams for two parallel current segments when $d \neq 0$ are shown.

Hence,

$$M = \int_0^{r_{12}} du \int_{b_1}^{cr_{34} + b_1} dw \frac{1}{r_p(u, w)},$$

where

$$w = c(v - b_2)$$

$$r_p(u, w) = ((u - w)^2 + d^2)^{1/2}$$

AI.2.1. When $d \neq 0$. The above definite integral is given by the indefinite integral

$$\int dx \int dy \frac{1}{r_p(x, y)} = g_p(x, y) + r_p(x, y),$$

where

$$g_p(x, y) = y \log(x - y + r_p(x, y)) + x \log(y - x + r_p(x, y)).$$

Therefore,

$$M = g_p(r_{12}, c(r_{34} - b_2)) + g_p(0, -cb_2) - g_p(r_{12}, -cb_2) - g_p(0, c(r_{34} - b_2)) \\ + r_{24} + r_{13} - r_{23} - r_{14}.$$

AI.2.2. When $d = 0$.

$$M = \int_0^{r_{12}} du \int_{b_1}^{cr_{34} + b_1} dw \frac{1}{|w - u|} \\ = |b_1 - r_{12}| \log |b_1 - r_{12}| + |cr_{34} + b_1| \log |cr_{34} + b_1| \\ - |b_1| \log |b_1| - |cr_{34} + b_1 - r_{12}| \log |cr_{34} + b_1 - r_{12}|.$$

REFERENCES

1. L. E. ALSOP, A. S. GOODMAN, F. G. GUSTAVSON, AND W. L. MIRANKER, *J. Comput. Phys.* **31**, 216 (1979).
2. W. H. CHANG, *IEEE Trans. Magn.* **MAG-17**, 764 (1981).
3. P. A. BRENNAN, N. RAVER AND A. E. RUEHLI, *IBM J. Res. Develop.* **23**, 661 (1979).
4. K. NISHI AND S. YAMAMOTO, "Measurement of 3D model inductance," Riken Symposium on Josephson Electronics, Wako, Saitama, March 18, 1986. [Japanese]